Two-potential parametrization to describe the pion vector form factor

A dispersive approach

Leon Heuser | HISKP, University of Bonn

in collaboration with G. Chanturia, C. Hanhart, M. Hoferichter, B. Kubis

Motivation

Current situation:

- Tension in the 2π data
- Differences in datasets are almost exclusively contained in inelastic contributions Stoffer et al. (2023)
- Inelastic effects are combined as a multiplicative factor in the current dispersive treatment Leplumey and Stoffer (2025)
- No unified fits available for multi-channel treatments Achasov and Kozhevnikov (2013)

Two-potential model: Hanhart (2012)

- Based on unitarity and analytic properties of the S-matrix
- Inelastic channels built explicitly and fit to data

Two-potential model: the concept

Model data with resonances (V_{R}) and non-resonant contribution (V_{B})

- Background should only be small part $\leftarrow$ VMD assumption
- Need T-matrix that corresponds to the potentials $V_{\mathrm{R/B}}$
- Sum of two unitary objects not unitary
  $\rightarrow$ T_{B} is unitary, T_{R} not unitary, $T_{\mathrm{tot}} = T_{\mathrm{B}} + T_{\mathrm{R}}$ unitary

---

$\Rightarrow$ Background dresses all resonant interactions

Two-potential model: diagrammatic representation

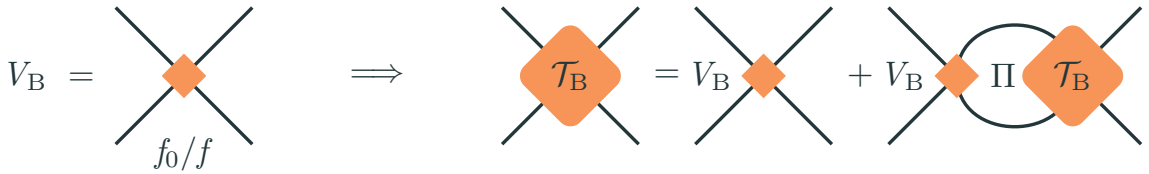

Two-potential model: diagrammatic representation

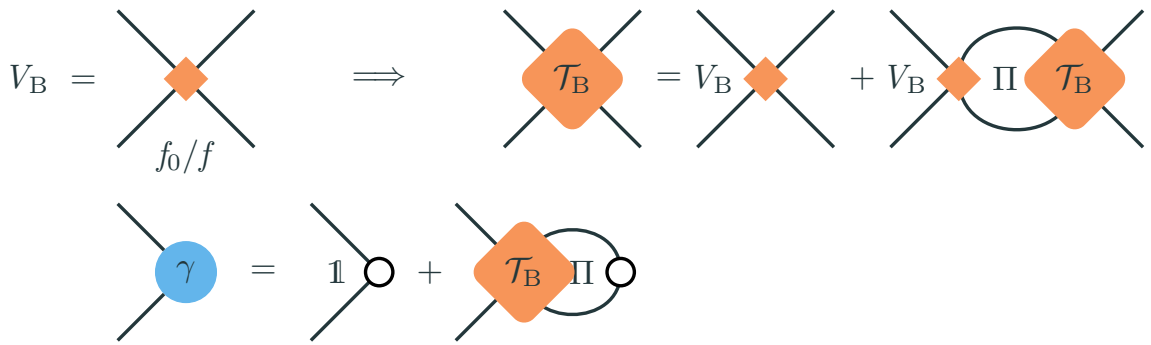

Two-potential model: diagrammatic representation

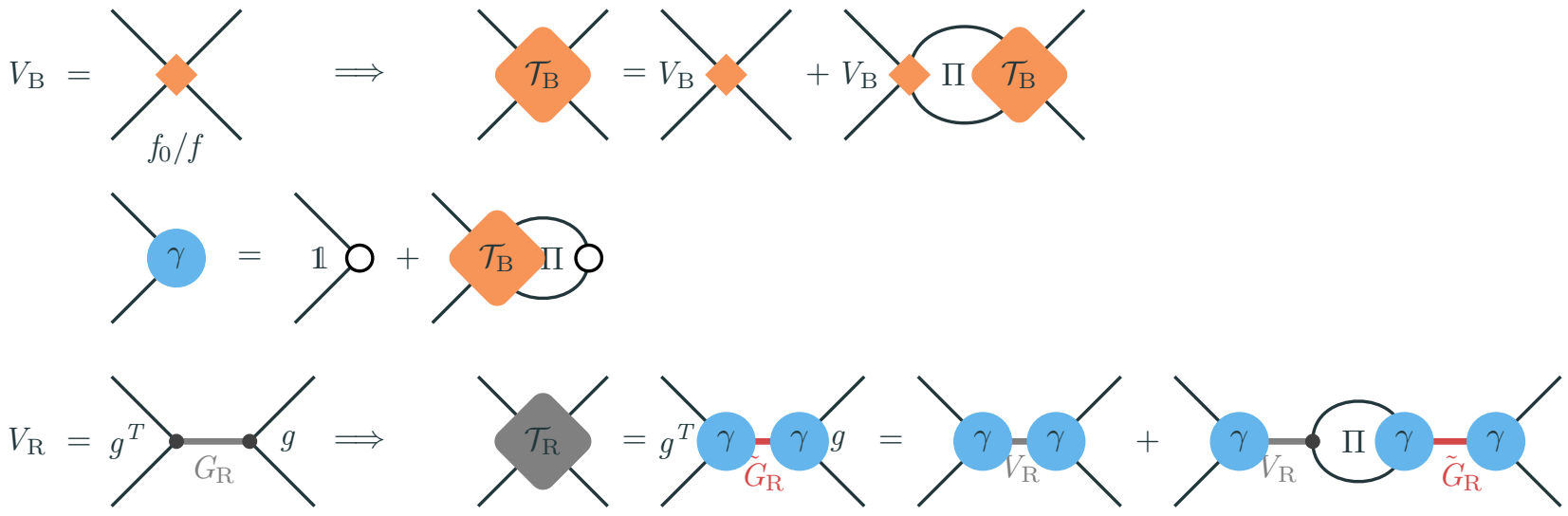

Two-potential model: diagrammatic representation

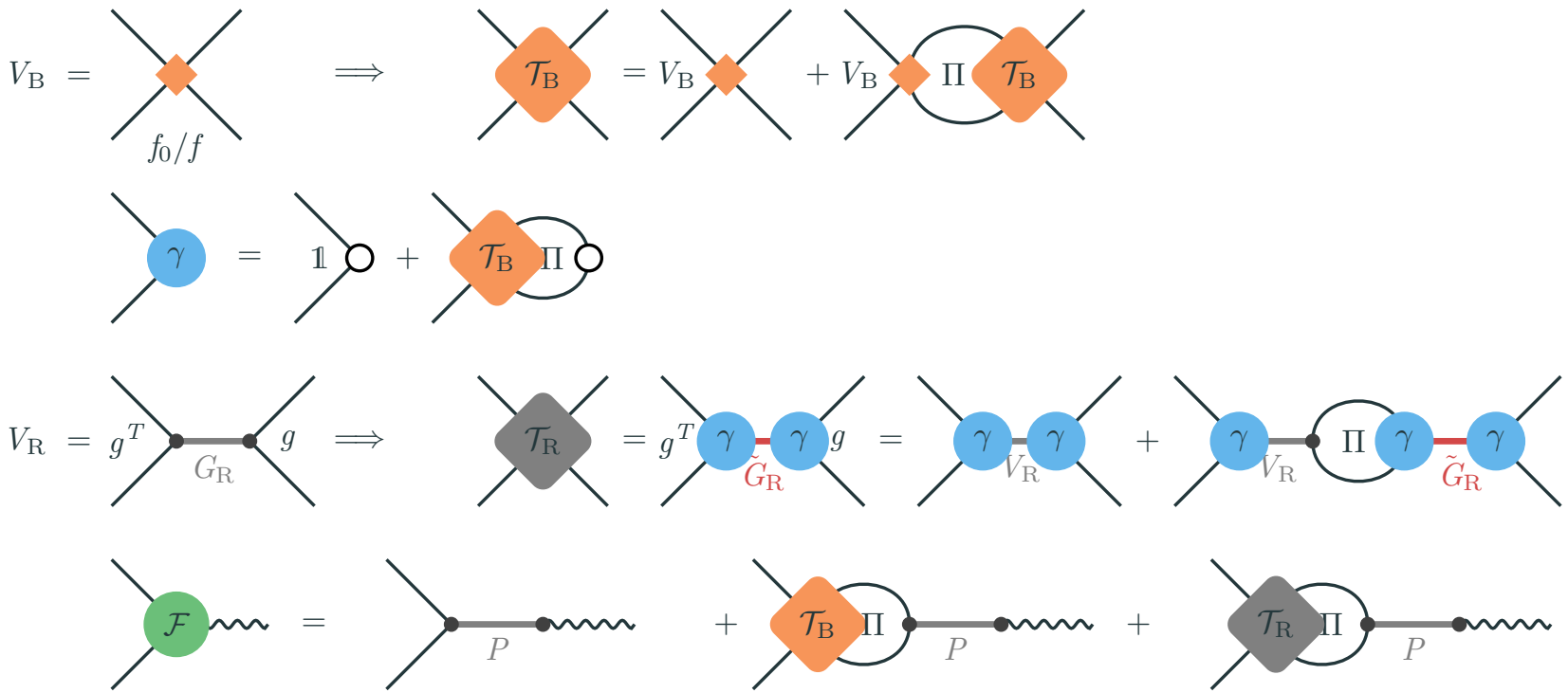

Two-potential model: formal representation

Background T-matrix

$$V_{\mathrm{B}}(s)_{ab} = f_{0,ab} \quad \Longrightarrow \quad \mathcal{T}_{\mathrm{B}} = (1 - V_{\mathrm{B}}\Pi)^{-1} V_{\mathrm{B}}$$

$$\text{with} \quad \Pi(s) = \frac{s}{\pi} \int_{s_{\mathrm{thr}}}^{\infty} \frac{\mathrm{d}s'}{s'} \frac{\rho(s')\xi(s')^2}{s' - s - i\epsilon} + const.$$

$$\gamma(s) = 1 + \mathcal{T}_{\mathrm{B}}(s)\Pi(s) \mathrel{\widehat{=}} p(s) \exp\left(\frac{s}{\pi} \int_{s_{\mathrm{thr}}}^{\infty} \frac{\mathrm{d}s'}{s'} \frac{\delta_{\mathrm{B}}(s')}{s' - s - i\epsilon} \right)$$

Two-potential model: formal representation

Background T-matrix

$$V_\mathrm{B}(s)_{ab} = f_{0,ab} \quad \Longrightarrow \quad \mathcal{T}_\mathrm{B} = \left(1 - V_\mathrm{B}\Pi\right)^{-1} V_\mathrm{B}$$

$$\text{with} \quad \Pi(s) = \frac{s}{\pi} \int_{s_\mathrm{thr}}^{\infty} \frac{\mathrm{d}s'}{s'} \frac{\rho(s')\xi(s')^2}{s' - s - i\epsilon} + \mathit{const.}$$

$$\gamma(s) = 1 + \mathcal{T}_\mathrm{B}(s)\Pi(s) \mathrel{\widehat{=}} p(s) \exp\left(\frac{s}{\pi} \int_{s_\mathrm{thr}}^{\infty} \frac{\mathrm{d}s'}{s'} \frac{\delta_\mathrm{B}(s')}{s' - s - i\epsilon}\right)$$

$$V_\mathrm{R}(s)_{ab} = \sum_{k=1}^{n_\mathrm{R}} \frac{g_a^k g_b^k}{m_k^2 - s} \quad \Longrightarrow \quad \mathcal{T}_\mathrm{R} = \gamma^\dagger \left(1 - V_\mathrm{R}\Sigma\right)^{-1} V_\mathrm{R}\gamma$$

Resonance T-matrix

$$\text{with} \quad \Sigma(s) = \frac{s}{\pi} \int_{s_\mathrm{thr}}^{\infty} \frac{\mathrm{d}s'}{s'} \frac{\rho(s')\xi(s')^2|\gamma(s')|^2}{s' - s - i\epsilon} + \mathit{const.}$$

$$\boxed{\mathcal{F} = \gamma \left(1 - V_\mathrm{R}\Sigma\right)^{-1} P} \quad \text{with} \quad P(s)_b = \sum_{k=1}^{n_\mathrm{R}} \frac{g_b^k a_k}{m_k^2 - s}$$

Form factor

Application to $\sigma(500), \rho(770)$: Heuser et al. (2024)

Vertex structures

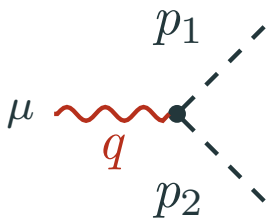

$$\sim \xi^{\mu}_{VPP} = (p_1 - p_2)^{\mu} \qquad (\text{for } \gamma^* \to \pi\pi, K\bar{K})$$

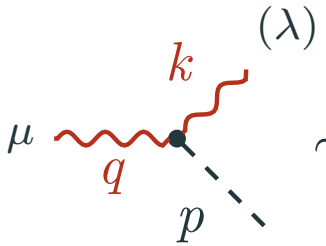

$$\sim \xi^{(\lambda)\mu}_{VVP} = \epsilon^{\mu\nu\alpha\beta} n^{(\lambda)}_{\nu} p_{\alpha} q_{\beta} \qquad (\text{for } \gamma^* \to \omega\pi^0, \rho\eta, K^*K)$$

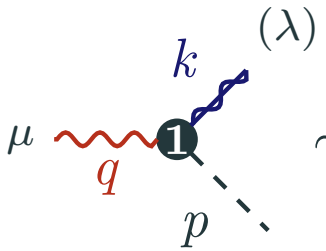

$$\sim \xi^{(\lambda)\mu}_{VAP,1} = (q \cdot k)\, n^{(\lambda)\mu} - (n^{(\lambda)} \cdot q)\, k^{\mu} \qquad (\text{for } \gamma^* \to a_1\pi)$$

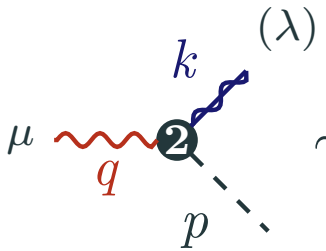

$$\sim \xi^{(\lambda)\mu}_{VAP,2} = q^2 k^2 n^{(\lambda)\mu} + (q \cdot k)(n^{(\lambda)} \cdot q) q^{\mu} - k^2 (n^{(\lambda)} \cdot q) q^{\mu}$$

Included channels ($J = 1$, $I = 1$)

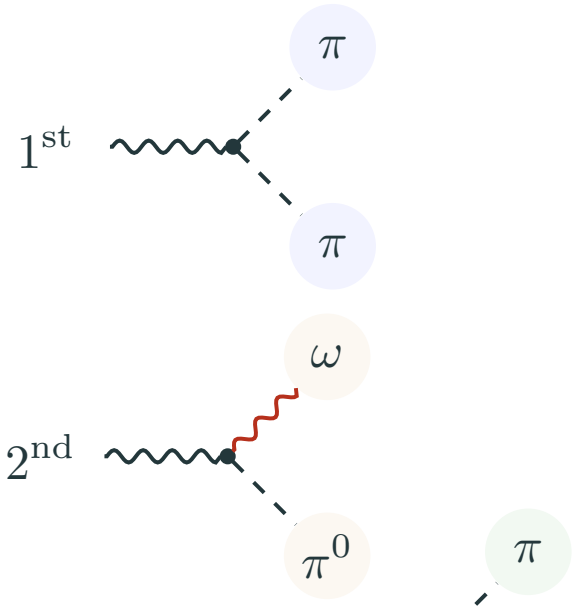

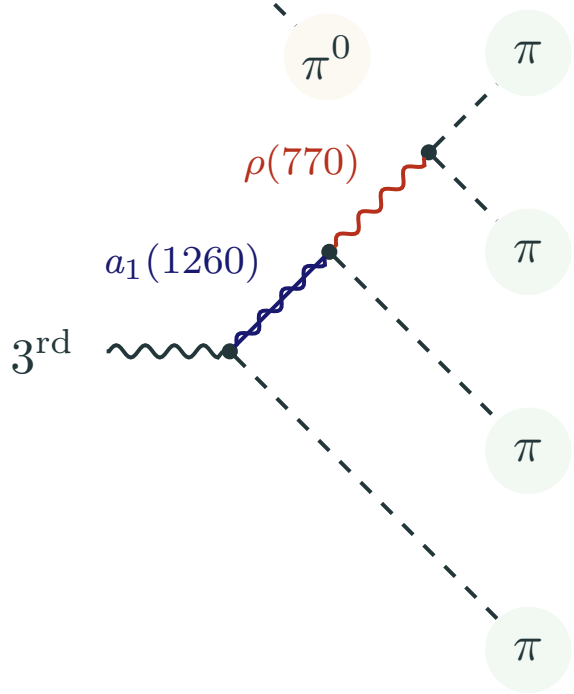

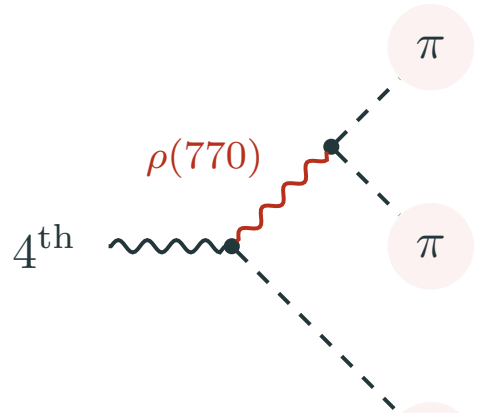

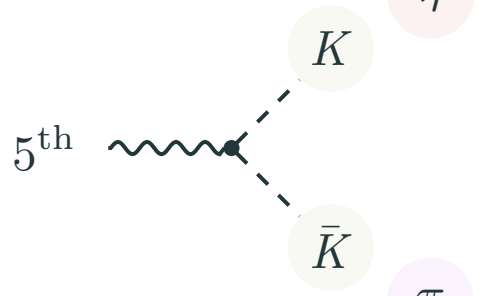

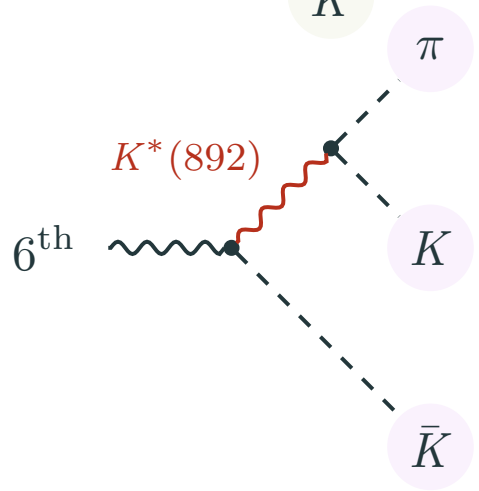

Semistable channels

Spectral function for an unstable state A via dressed propagator
$\rightarrow$ fix parameters g, M_A like in Heuser et al. (2024) via pole position

$$\sigma_A(q^2) = -\frac{1}{\pi}\mathrm{Im}\left(G_A(q^2)\right) , \quad \text{where} \quad G_A(q^2) = \frac{1}{q^2 - M_A^2 + g^2\Pi_i(q^2)}$$

Imaginary part of the self-energy Π_{AB} with A being a (broad) resonance

$$\mathrm{Im}\Pi_{AB} = \int_{s_{\mathrm{thr,decay}}}^{(\sqrt{s}-M_B)^2} \mathrm{d}q_A^2 \rho(s, q_A^2, M_B^2)\xi^2(s, q_A^2, M_B^2)\sigma_A(q_A^2)$$

$$\mathrm{Im}\Pi_{\pi\pi\eta}(s) = \int_{(2M_\pi)^2}^{(\sqrt{s}-M_\eta)^2} \mathrm{d}q_\rho^2 \, \sigma_\rho(q_\rho^2)\rho(s, q_\rho^2, M_\eta^2) \, \xi_{VVP}^2(s, q_\rho^2, M_\eta^2)$$

$$\mathrm{Im}\Pi_{\pi KK}(s) = \int_{(M_\pi+M_K)^2}^{(\sqrt{s}-M_K)^2} \mathrm{d}q_{K^*}^2 \, \sigma_{K^*}(q_{K^*}^2)\rho(s, q_{K^*}^2, M_K^2)\xi_{VVP}^2(s, q_{K^*}^2, M_K^2)$$

Semistable channels: 4π and the a_1 spectral function

$a_1\pi$ problematic:

a_1 pole might be model dependent + three-body effects

$\rightarrow$ use τ-decay data for a_1 and fit $g_{a_1\rho\pi}$, M_{a_1}

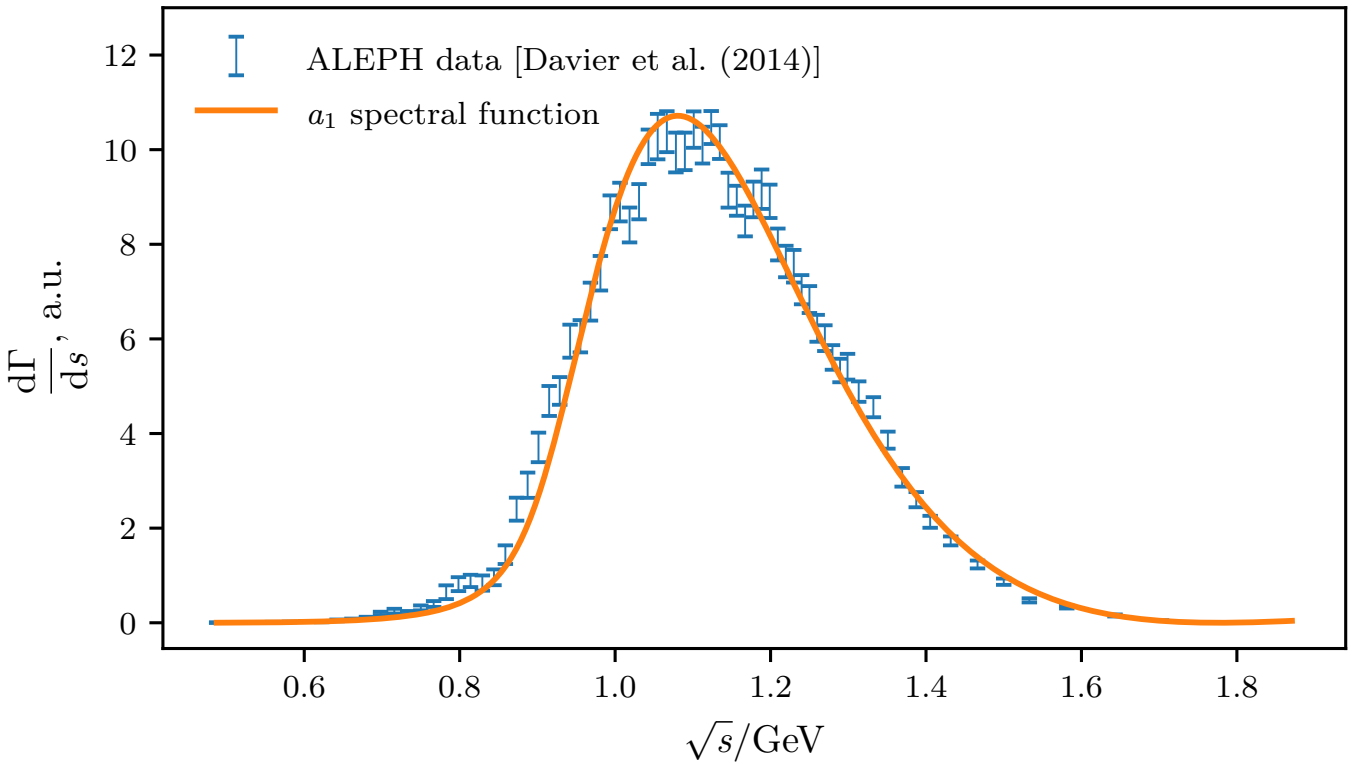

Semistable channels: 4π and the a_1 spectral function

$a_1\pi$ problematic:
difference between interference effects in $2\pi^0\pi^+\pi^-$ and $2(\pi^+\pi^-)$ not accounted for within the model
$\rightarrow$ fit multiplicative factor to ratio of corresponding cross sections

$$r_{N/C}(s) = \frac{1}{2}\left(1 + \exp^{-1}\left(\frac{a^2 - s}{b^2}\right)\right)$$

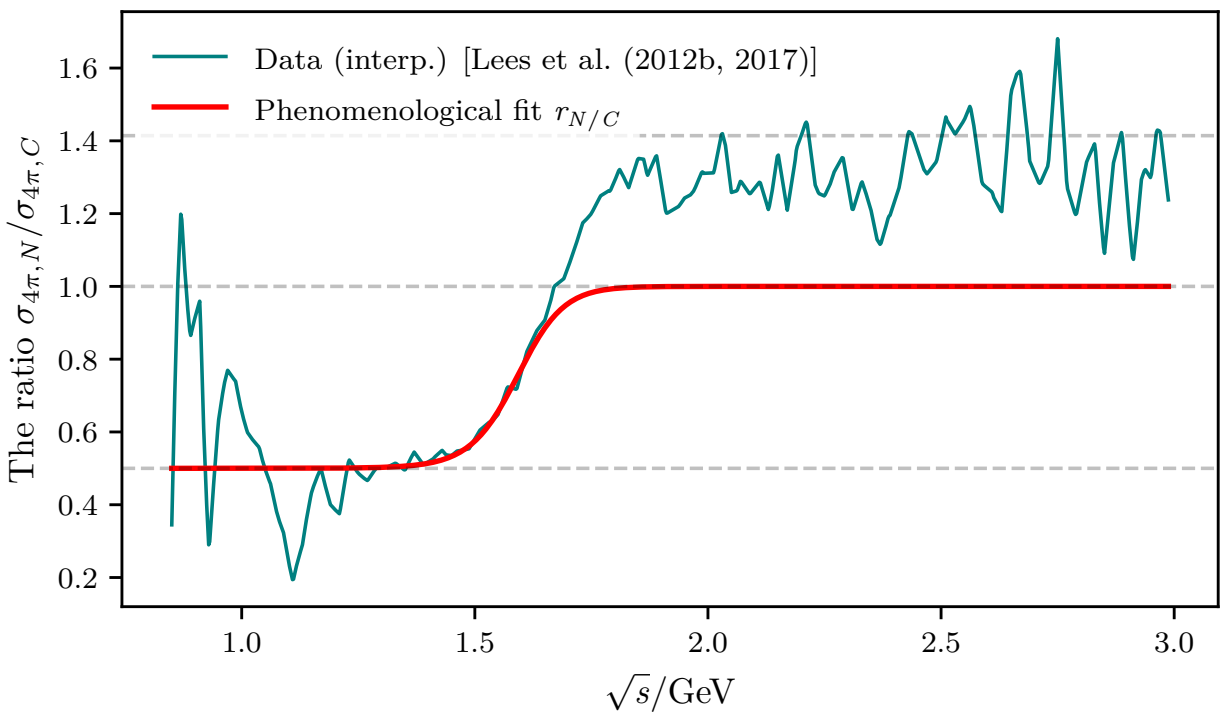

Semistable channels: 4π and the a_1 spectral function

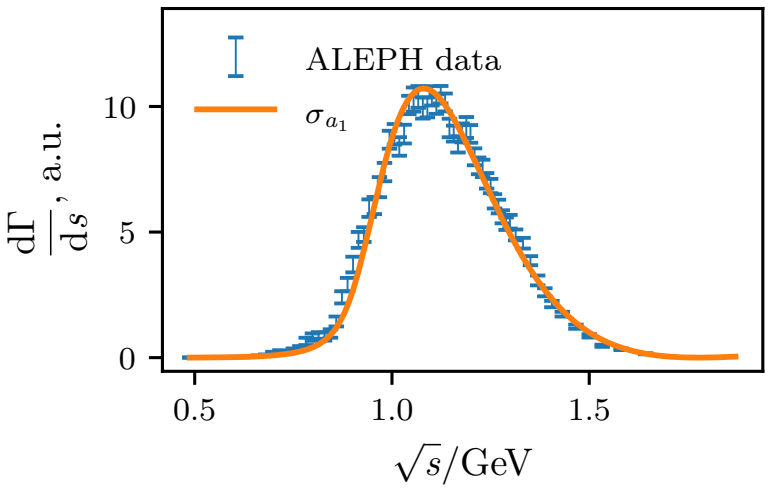

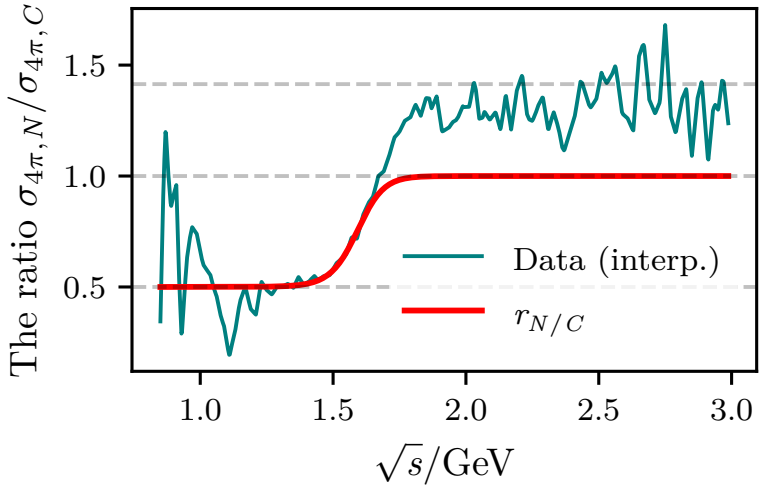

$$\mathrm{Im}\Pi_{\rho\pi}(q_{a_1}^2) = \int_{(2M_\pi)^2}^{(\sqrt{q_{a_1}^2}-M_\pi)^2} \mathrm{d}q_\rho^2\, \sigma_\rho(q_\rho^2)\, \rho(q_{a_1}^2, q_\rho^2, M_\pi^2)\, \xi_{VVP}^2(q_{a_1}^2, q_\rho^2, M_\pi^2)$$

$$\sigma_{a_1}(q_{a_1}^2) = -\frac{1}{\pi}\mathrm{Im}\left(\frac{1}{q_{a_1}^2 - M_{a_1}^2 + g_{a_1\rho\pi}^2\Pi_{\rho\pi}(q_{a_1}^2)}\right)$$

$$\mathrm{Im}\Pi_{i,4\pi}(s) = \int_{(3M_\pi)^2}^{(\sqrt{s}-M_\pi)^2} \mathrm{d}q_{a_1}^2\, \sigma_{a_1}(q_{a_1}^2)\, \rho(s, q_{a_1}^2, M_\pi^2)\, \xi_{i,VAP}^2(s, q_{a_1}^2, M_\pi^2)\, r_{N/C}(s)$$

Model is set up – what now?

The fully set-up model can be used to

- test compatibility of data sets
- understand the complex plane
- extract poles and residues

For all of this: we need to fit!

Parameters	**3 resonances**	**4 resonances**
Background parameters $f_{0,ij}$	28	28
Resonance masses m_k	3	4
Source couplings a_k	3	4
Resonance couplings g_i^k	21	28
Total	**59**	**68**

+ parameters from isospin-breaking effects (see e.g. slide 19 below)

Backup slides

Semistable channels: 4π and the a_1 spectral function

$a_1\pi$ problematic: two structures $\xi_{VAP,1}$ and $\xi_{VAP,2}$ for $V \to AP$
Want no interference between form factors to isolate $\mathrm{Im}(\Pi_{4\pi})$ clearly
$\to$ rotate into suitable basis

$$\sigma^{(0)}_{e^+e^-\to 4\pi}(s) = \left(\frac{e^2}{s}\right)^2 \left[\mathrm{Im}\Pi_{4\pi,1}(s)|f^{(1)}_{a_1\pi}(s)|^2 + \mathrm{Im}\Pi_{4\pi,2}(s)|f^{(2)}_{a_1\pi}(s)|^2\right]$$

$\Rightarrow$ $a_1\pi$ is split into two channels

The pion vector form factor with explicit inelasticities

Fitting strategy and preliminary results

George Chanturia | HISKP, University of Bonn

in collaboration with L. A. Heuser, C. Hanhart, M. Hoferichter, B. Kubis

Simultaneous fit to data

$\pi^+\pi^-$ production: BaBar [Lees et al. (2012a)],
KLOE [Anastasi et al. (2018)], CMD-3 [Ignatov et al. (2024)]

$\pi\pi$ p-wave phase shift: Bern [Colangelo (2004), ..., Stoffer et al. (2023), ...]

$\pi^0\omega$ production: BaBar [Lees et al. (2017)],
CMD-2 [Akhmetshin et al. (2003)], SND [Achasov et al. (2000, 2016)]

ω decay: NA60 [Arnaldi et al. (2009, 2016)]

4π production: BaBar [Lees et al. (2012b, 2017)]

Kaon VFF from τ decay: BaBar [Lees et al. (2018)]

$\pi\pi\eta$ production: BaBar [Aubert et al. (2007)],
CMD-2 [Akhmetshin et al. (2000)], SND [Aulchenko et al. (2015)]

$KK\pi$ production: BaBar [Aubert et al. (2008)]

Radiative decay widths for $V \to P\gamma$: PDG [Takahashi et al. (2026)]

a_1 spectral function from τ decay: ALEPH [Davier et al. (2014)]

Simultaneous fit to data

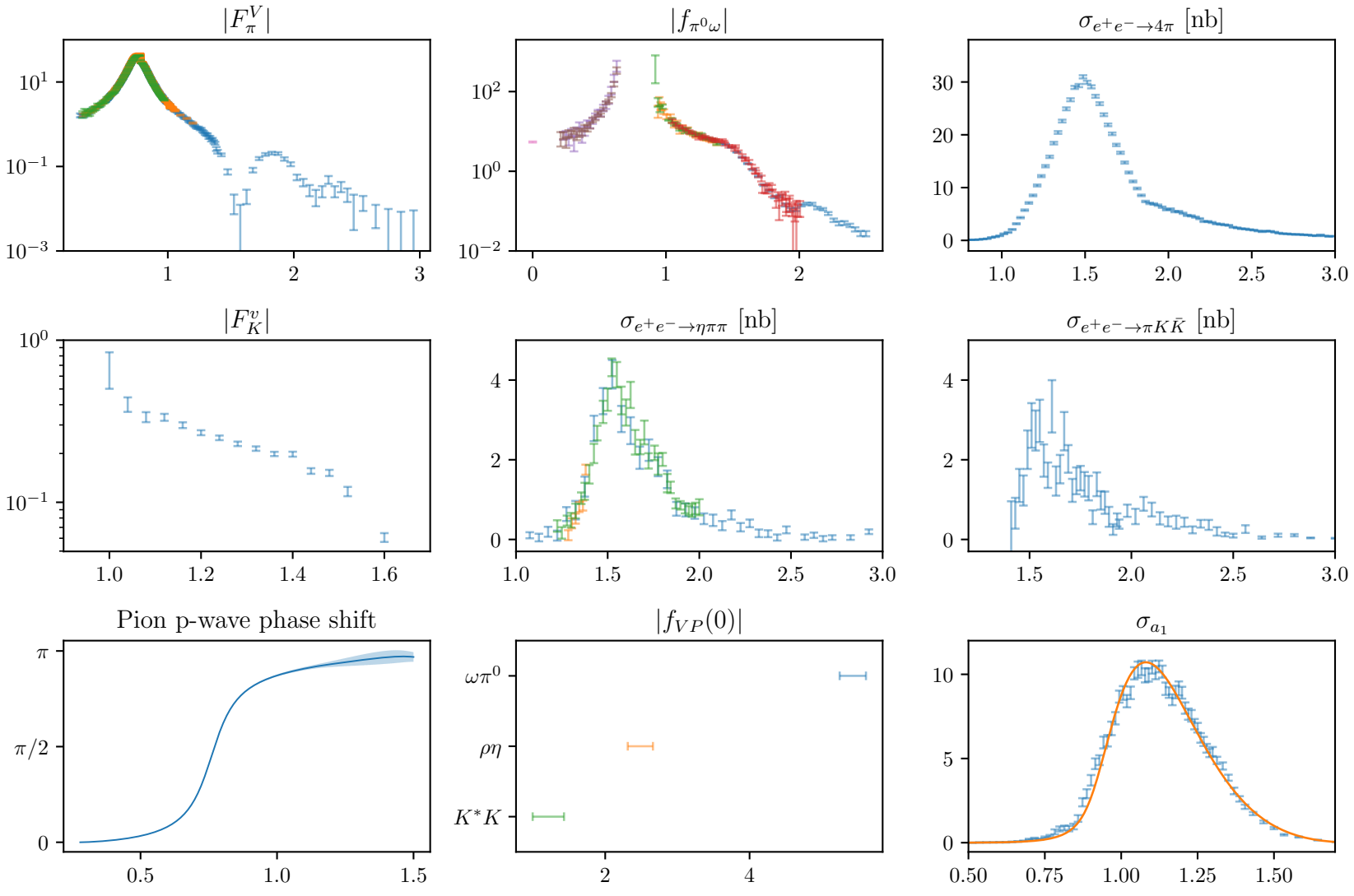

Simultaneous fit to data: model performance

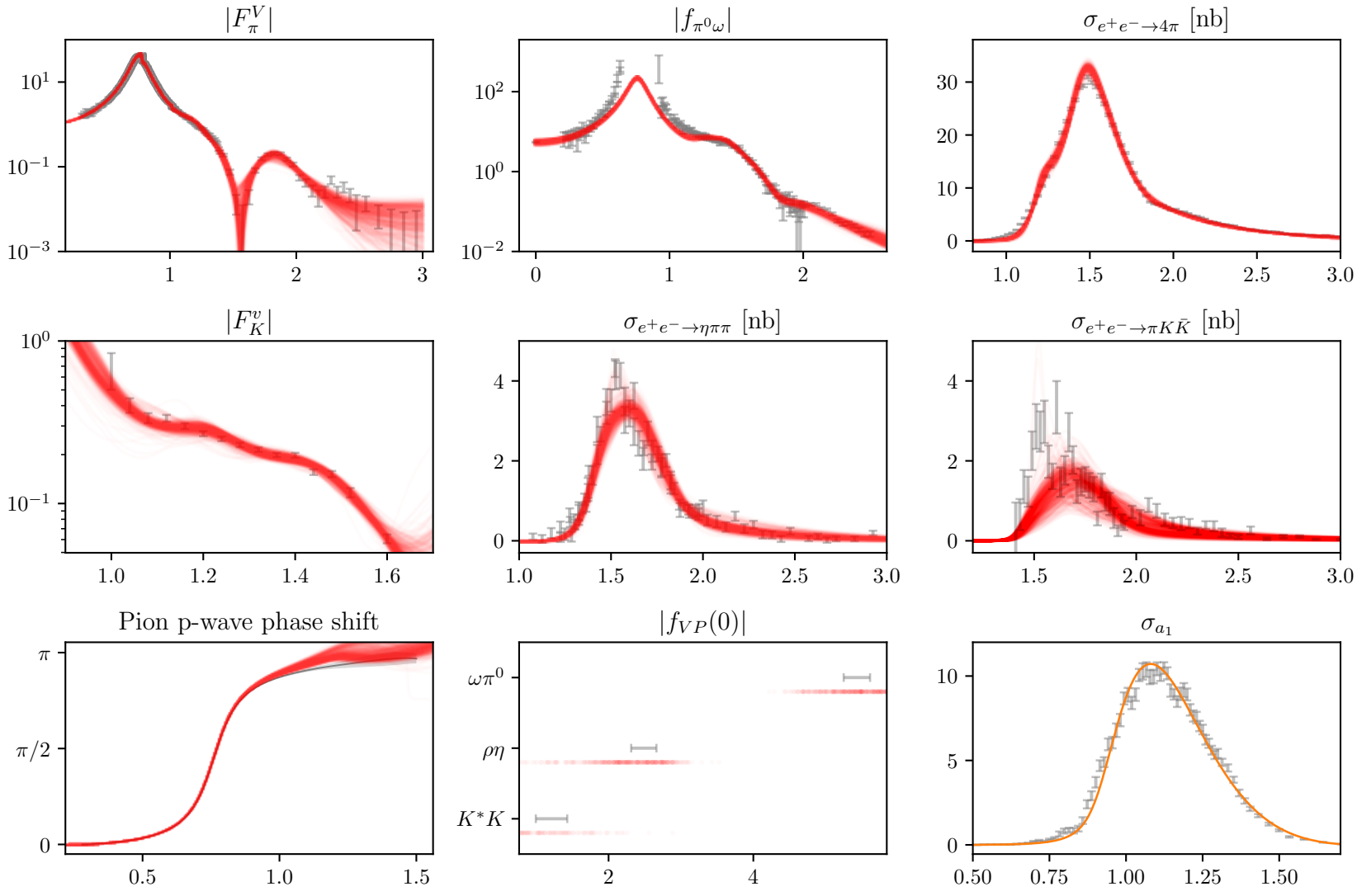

Challenges and strategies

- Large number of parameters
  $\Longrightarrow$ must be careful with local minima
  $\Longrightarrow$ both gradient-based and global minimization routines
- Risk of overfitting
  $\Longrightarrow$ lowest number of resonances (ρ, ρ', ρ'')
  $\Longrightarrow$ diagonal background preferable
- Asymptotic behaviour not built in
  $\Longrightarrow$ must be imposed: punishing factors and post-processing
- Narrow (unphysical) resonances occur as fit artefacts
  $\Longrightarrow$ must be filtered out in the post-processing step
- Data quality not uniform
  $\Longrightarrow$ must be compensated for during fitting
- Pion VFF sensitive to phase shifts, ω parameters
  $\Longrightarrow$ individual input for different datasets
- Need to correct for bias
  $\Longrightarrow$ d'Agostini procedure (see e.g. Ball et al. (2010))

Contributions to the global $\bar{\chi}^2$

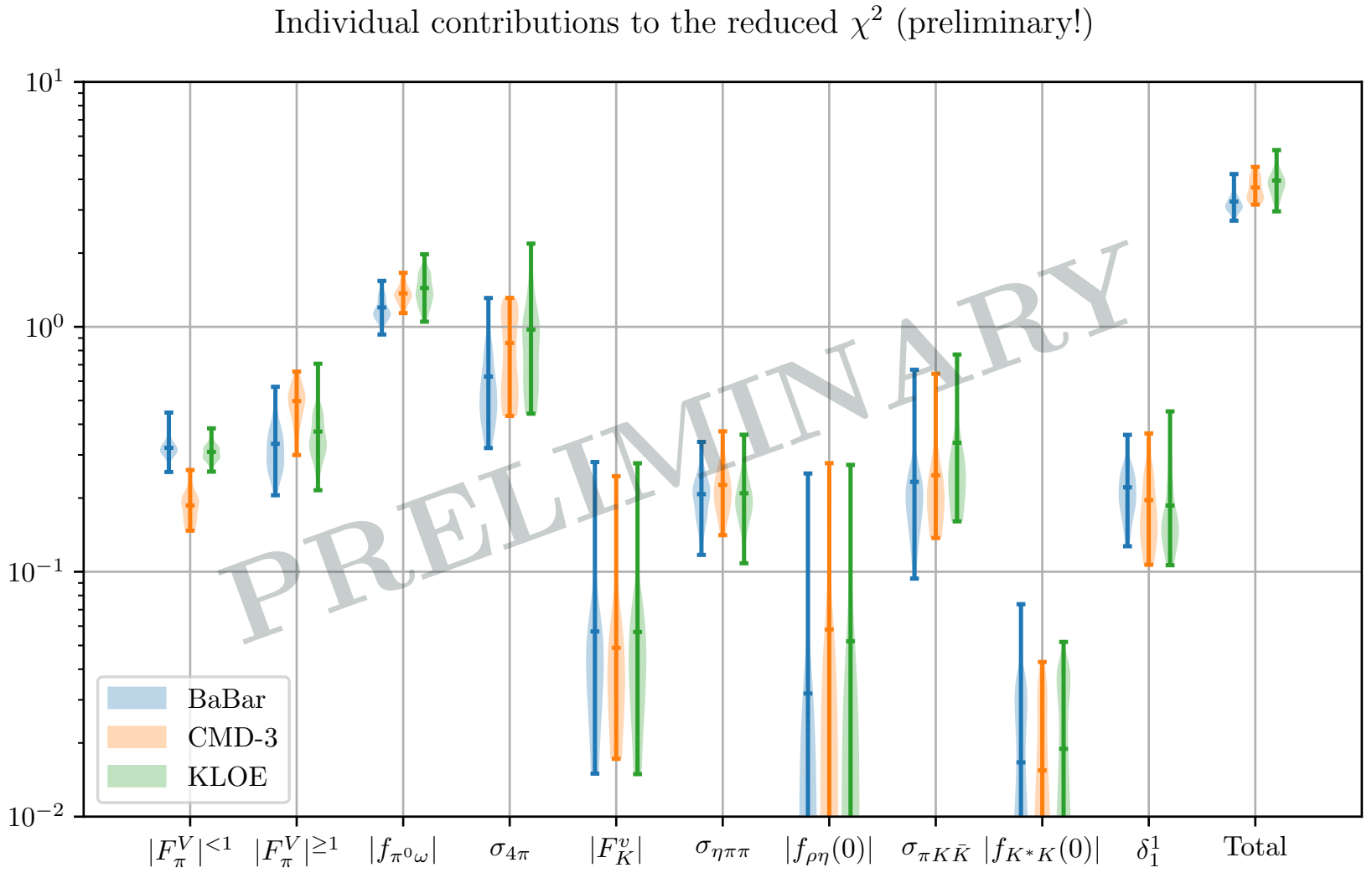

$\pi\pi$ fits below 1 GeV

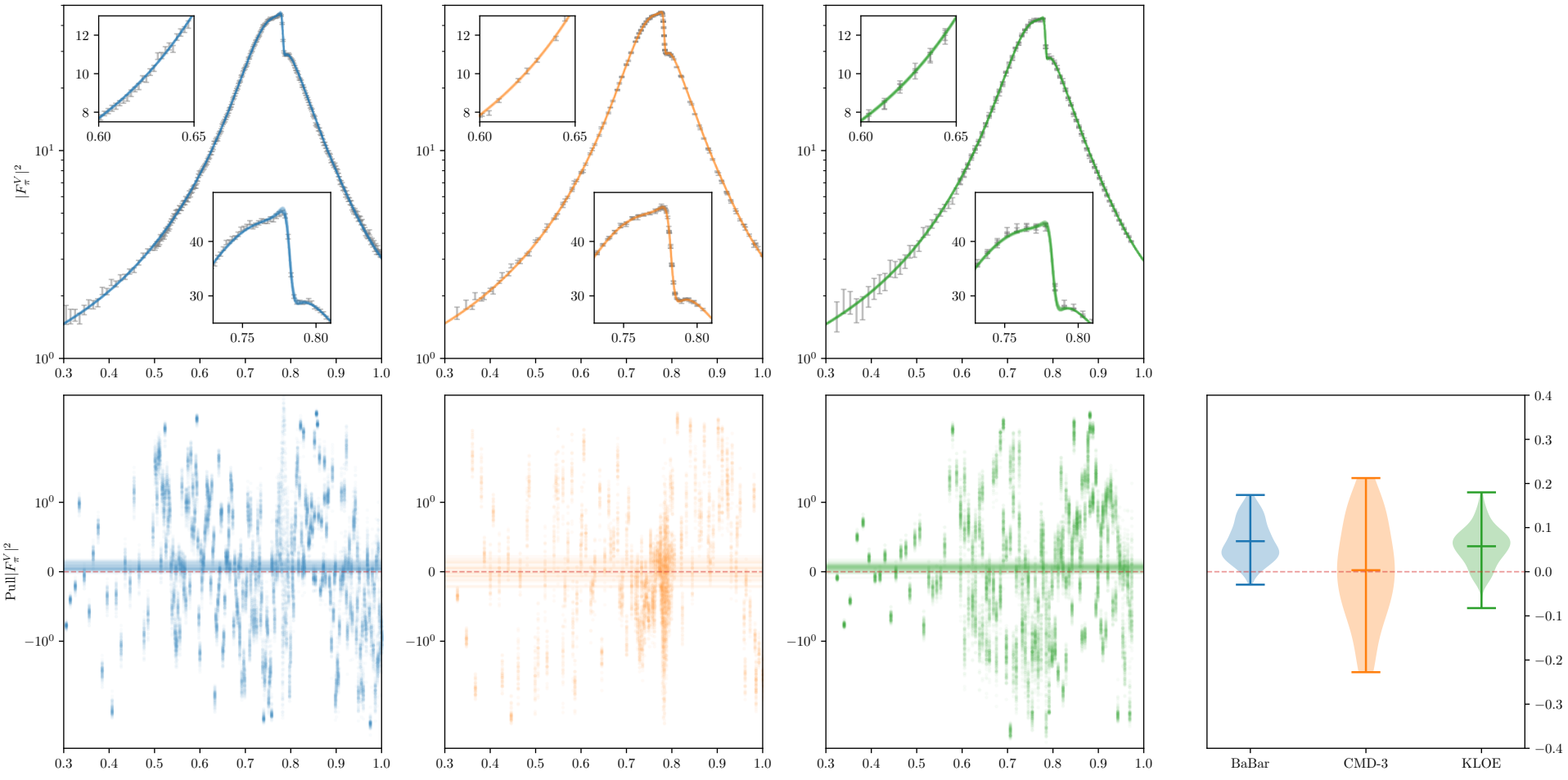

ω parameters from 2-pion data

$$F_\pi^V(s) = \left(1 + \kappa_\omega \frac{s}{s - M_\omega^2 + iM_\omega\Gamma_\omega} + \dots\right) F_\pi^{V,I=1}(s)$$

- Γ_ω fixed from 3π Hoferichter et al. (2023)
- Bounds for M_ω and κ_ω were selected according to the $\pi\pi$ dataset [Stoffer et al. (2023)]

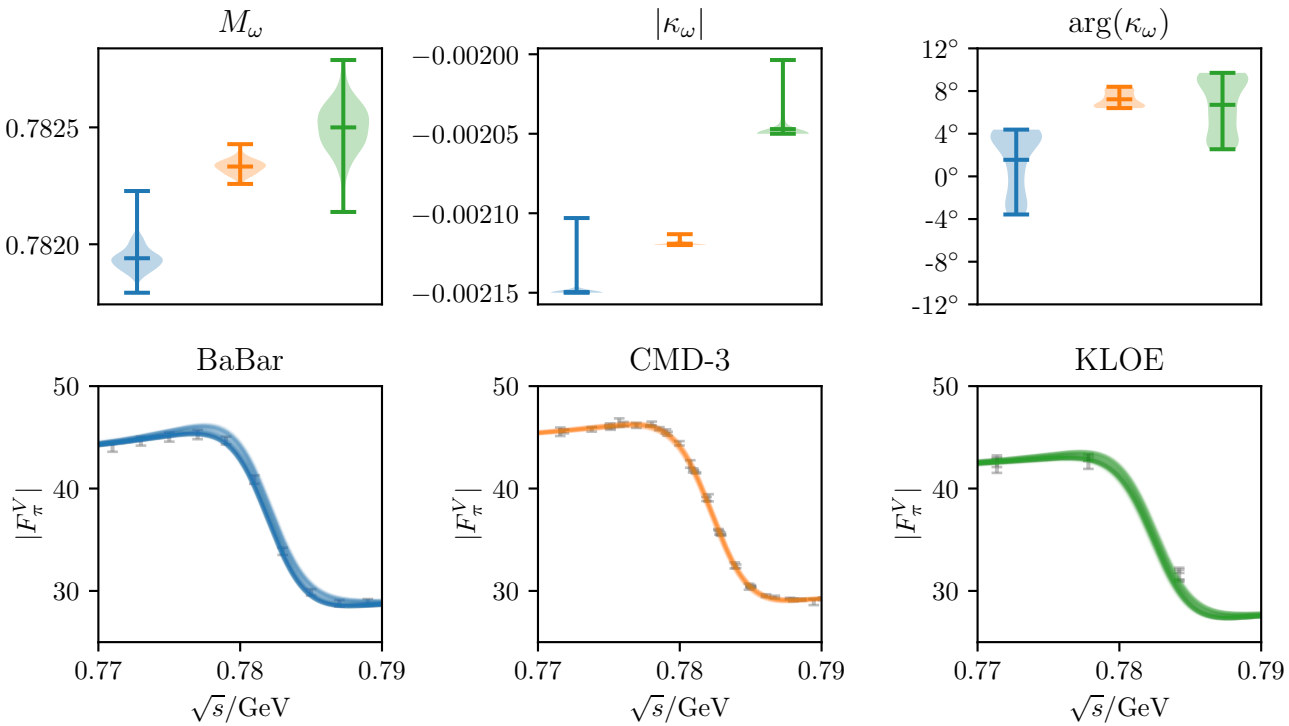

Summary

- Global fits performed to data from multiple channels.
- Dispersive constraints imposed through $\pi\pi$-specific phases.
- Two-potential formalism ensures unitarity and analyticity.
- Preliminary analysis shows noticeable differences in the quality of fit between the pion production datasets.
- Early evidence suggests that CMD-3 leads to better consistency with data for inelastic channels.
- **Quantification of significance currently under study** (stay tuned for the publication!).

Backup slides

Fits with diagonal background

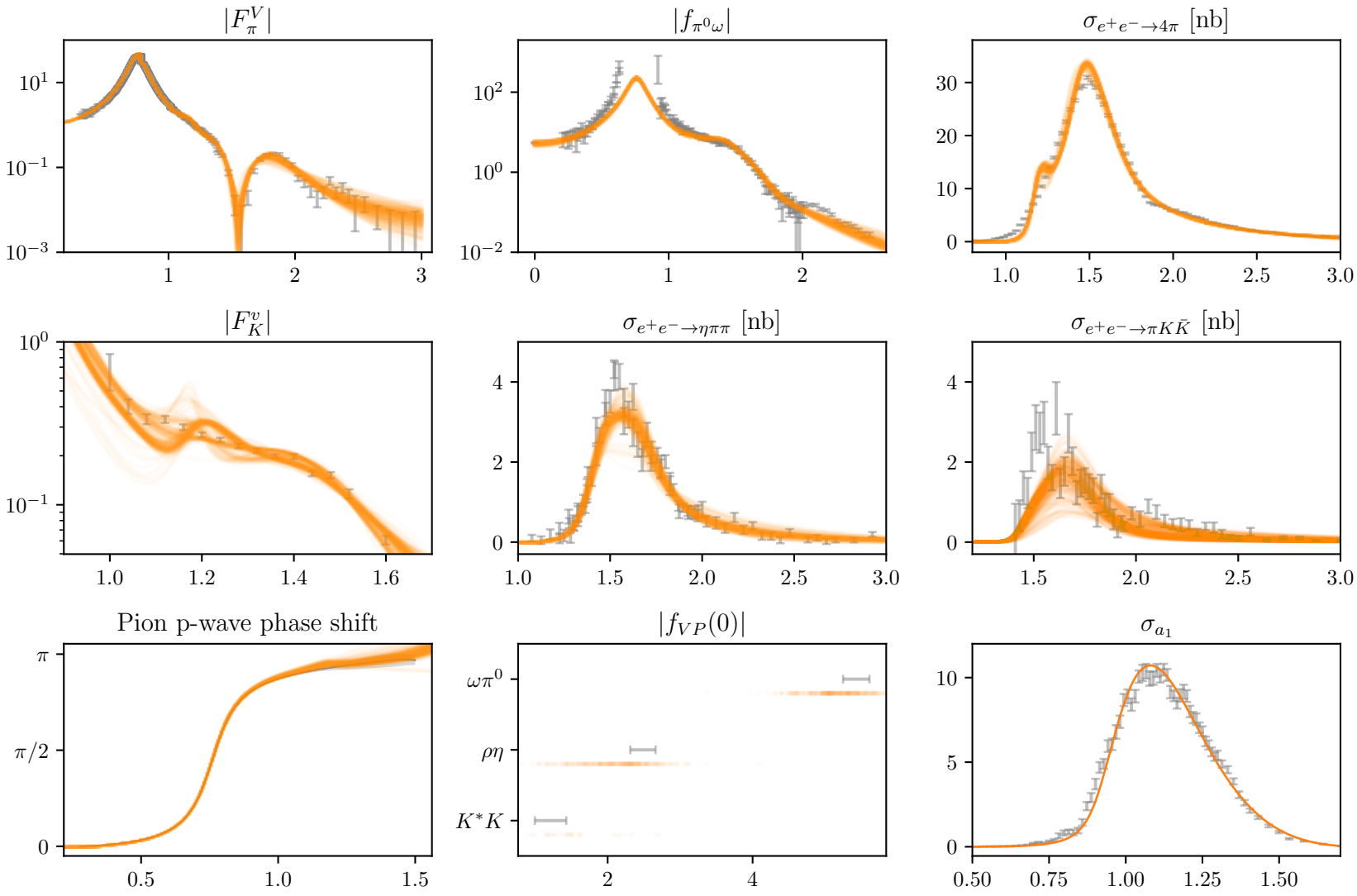

Fits with diagonal background, $\pi\pi$ favoured

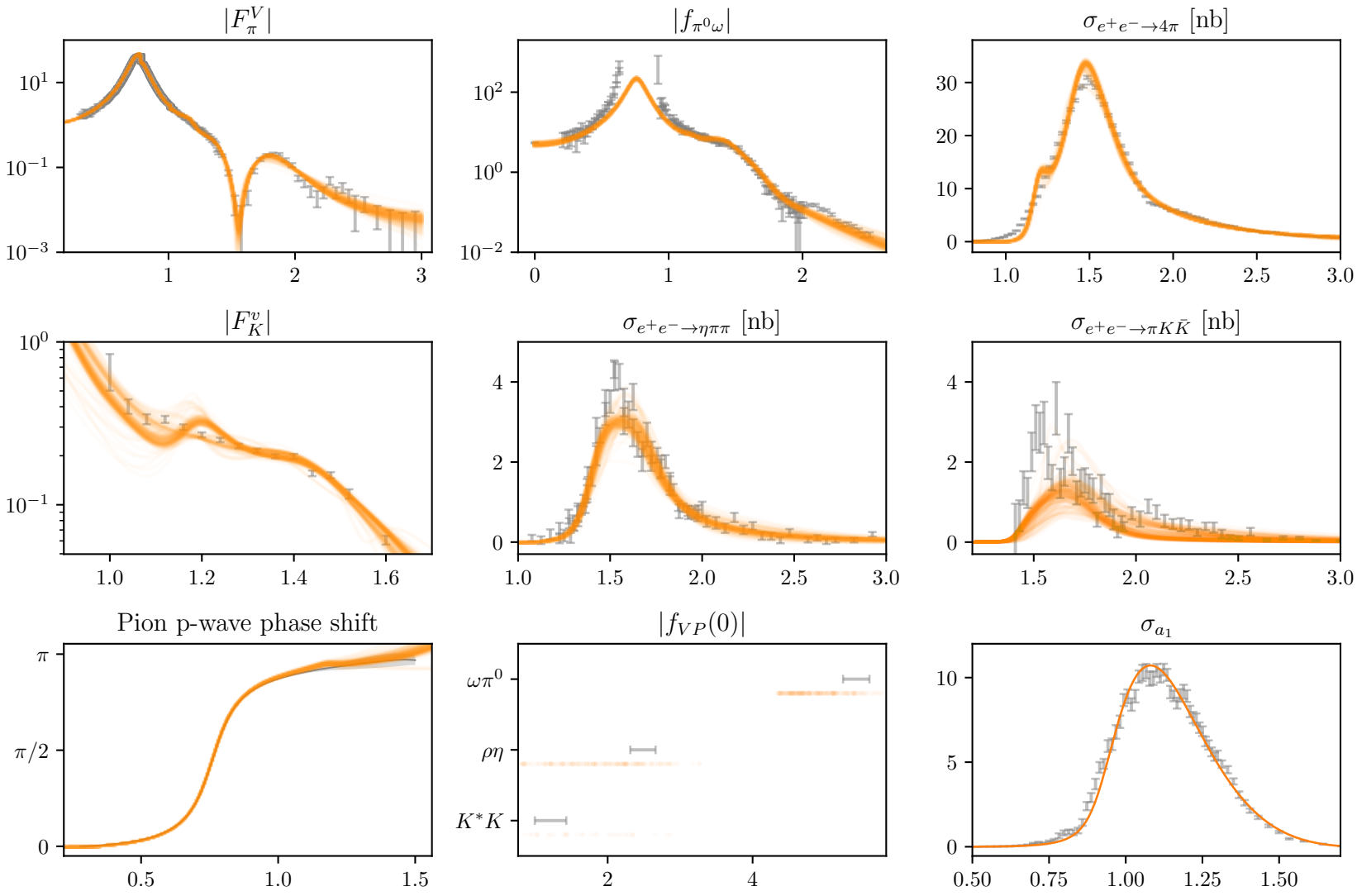

$\bar{\chi}^2$, diagonal background

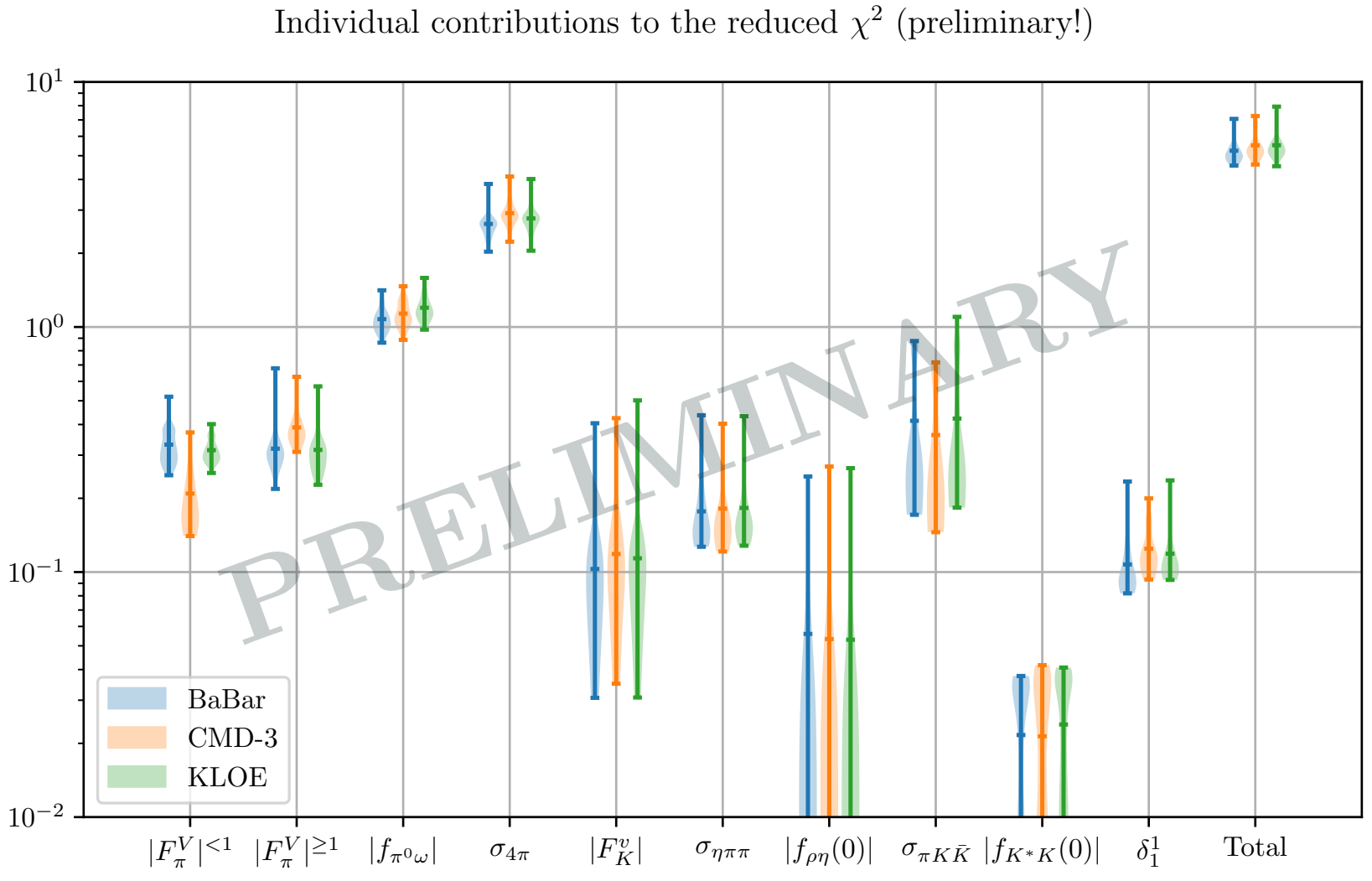

References

M. N. Achasov et al. The Process $e^+e^- \to \omega\pi^0 \to \pi^0\pi^0\gamma$ up to 1.4 GeV. *Phys. Lett. B*, 486:29–34, 2000. doi: 10.1016/S0370-2693(00)00706-1.

M. N. Achasov et al. Updated measurement of the $e^+e^- \to \omega\pi^0 \to \pi^0\pi^0\gamma$ cross section with the SND detector. *Phys. Rev. D*, 94(11):112001, 2016. doi: 10.1103/PhysRevD.94.112001.

N. N. Achasov and A. A. Kozhevnikov. Pion form factor and reactions $e^+e^- \to \omega\pi^0$ and $e^+e^- \to \pi^+\pi^-\pi^+\pi^-$ at energies up to 2–3 GeV in the many-channel approach. *Phys. Rev. D*, 88(9): 093002, 2013. doi: 10.1103/PhysRevD.88.093002.

References ii

R. R. Akhmetshin et al. Study of the process $e^+e^- \to \pi^+\pi^-\pi^+\pi^-\pi^0$ with CMD-2 detector. *Phys. Lett. B*, 489:125–130, 2000. doi: 10.1016/S0370-2693(00)00937-0.

R. R. Akhmetshin et al. Study of the process $e^+e^- \to \omega\pi^0 \to \pi^0\pi^0\gamma$ in c.m. energy range 920 MeV–1380 MeV at CMD-2. *Phys. Lett. B*, 562:173–181, 2003. doi: 10.1016/S0370-2693(03)00595-1.

A. Anastasi et al. Combination of KLOE $\sigma\left(e^+e^- \to \pi^+\pi^-\gamma(\gamma)\right)$ measurements and determination of $a_\mu^{\pi^+\pi^-}$ in the energy range $0.10 < s < 0.95$ GeV^2. *JHEP*, 03:173, 2018. doi: 10.1007/JHEP03(2018)173.

R. Arnaldi et al. Study of the electromagnetic transition form-factors in $\eta \to \mu^+\mu^-\gamma$ and $\omega \to \mu^+\mu^-\pi^0$ decays with NA60. *Phys. Lett. B*, 677:260–266, 2009. doi: 10.1016/j.physletb.2009.05.029.

References iii

R. Arnaldi et al. Precision study of the $\eta \to \mu^+\mu^-\gamma$ and $\omega \to \mu^+\mu^-\pi^0$ electromagnetic transition form-factors and of the $\rho \to \mu^+\mu^-$ line shape in NA60. *Phys. Lett. B*, 757:437–444, 2016. doi: 10.1016/j.physletb.2016.04.013.

Bernard Aubert et al. The $e^+e^- \to 2(\pi^+\pi^-)\pi^0$, $2(\pi^+\pi^-)\eta$, $K^+K^-\pi^+\pi^-\pi^0$ and $K^+K^-\pi^+\pi^-\eta$ Cross Sections Measured with Initial-State Radiation. *Phys. Rev. D*, 76:092005, 2007. doi: 10.1103/PhysRevD.76.092005. [Erratum: Phys.Rev.D 77, 119902 (2008)].

Bernard Aubert et al. Measurements of $e^+e^- \to K^+K^-\eta$, $K^+K^-\pi^0$ and $K^0_s K^\pm\pi^\mp$ cross- sections using initial state radiation events. *Phys. Rev. D*, 77:092002, 2008. doi: 10.1103/PhysRevD.77.092002.

References iv

V. M. Aulchenko et al. Measurement of the $e^+e^- \to \eta\pi^+\pi^-$ cross section in the center-of-mass energy range 1.22-2.00 GeV with the SND detector at the VEPP-2000 collider. *Phys. Rev. D*, 91(5): 052013, 2015. doi: 10.1103/PhysRevD.91.052013.

Richard D. Ball, Luigi Del Debbio, Stefano Forte, Alberto Guffanti, Jose I. Latorre, Juan Rojo, and Maria Ubiali. Fitting Parton Distribution Data with Multiplicative Normalization Uncertainties. *JHEP*, 05:075, 2010. doi: 10.1007/JHEP05(2010)075.

Gilberto Colangelo. Hadronic contributions to a(mu) below one-GeV. *Nucl. Phys. B Proc. Suppl.*, 131:185–191, 2004. doi: 10.1016/j.nuclphysbps.2004.02.025.

References v

Michel Davier, Andreas Höcker, Bogdan Malaescu, Chang-Zheng Yuan, and Zhiqing Zhang. Update of the ALEPH non-strange spectral functions from hadronic τ decays. *Eur. Phys. J. C*, 74(3): 2803, 2014. doi: 10.1140/epjc/s10052-014-2803-9.

C. Hanhart. A New Parameterization for the Pion Vector Form Factor. *Phys. Lett. B*, 715:170–177, 2012. doi: 10.1016/j.physletb.2012.07.038.

L. A. Heuser, G. Chanturia, F. K. Guo, C. Hanhart, M. Hoferichter, and B. Kubis. From pole parameters to line shapes and branching ratios. *Eur. Phys. J. C*, 84(6):599, 2024. doi: 10.1140/epjc/s10052-024-12884-6.

References vi

Martin Hoferichter, Bai-Long Hoid, Bastian Kubis, and Dominic Schuh. Isospin-breaking effects in the three-pion contribution to hadronic vacuum polarization. *JHEP*, 08:208, 2023. doi: 10.1007/JHEP08(2023)208.

F. V. Ignatov et al. Measurement of the $e^+e^- \to \pi^+\pi^-$ cross section from threshold to 1.2 GeV with the CMD-3 detector. *Phys. Rev. D*, 109(11):112002, 2024. doi: 10.1103/PhysRevD.109.112002.

J. P. Lees et al. Precise Measurement of the $e^+e^- \to \pi^+\pi^-(\gamma)$ Cross Section with the Initial-State Radiation Method at BABAR. *Phys. Rev. D*, 86:032013, 2012a. doi: 10.1103/PhysRevD.86.032013.

J. P. Lees et al. Initial-State Radiation Measurement of the $e^+e^- \to \pi^+\pi^-\pi^+\pi^-$ Cross Section. *Phys. Rev. D*, 85:112009, 2012b. doi: 10.1103/PhysRevD.85.112009.

References vii

J. P. Lees et al. Measurement of the $e^+e^- \to \pi^+\pi^-\pi^0\pi^0$ cross section using initial-state radiation at BABAR. *Phys. Rev. D*, 96(9): 092009, 2017. doi: 10.1103/PhysRevD.96.092009.

J. P. Lees et al. Measurement of the spectral function for the $\tau^- \to K^- K_S \nu_\tau$ decay. *Phys. Rev. D*, 98(3):032010, 2018. doi: 10.1103/PhysRevD.98.032010.

Thomas P. Leplumey and Peter Stoffer. Dispersive analysis of the pion vector form factor without zeros. 2025.

Peter Stoffer, Gilberto Colangelo, and Martin Hoferichter. Puzzles in the hadronic contributions to the muon anomalous magnetic moment. *JINST*, 18(10):C10021, 2023. doi: 10.1088/1748-0221/18/10/C10021.

F. Takahashi et al. Review of Particle Physics. *Int. J. Mod. Phys. A*, 41:2630011, 2026. doi: 10.1142/S0217751X26300115.